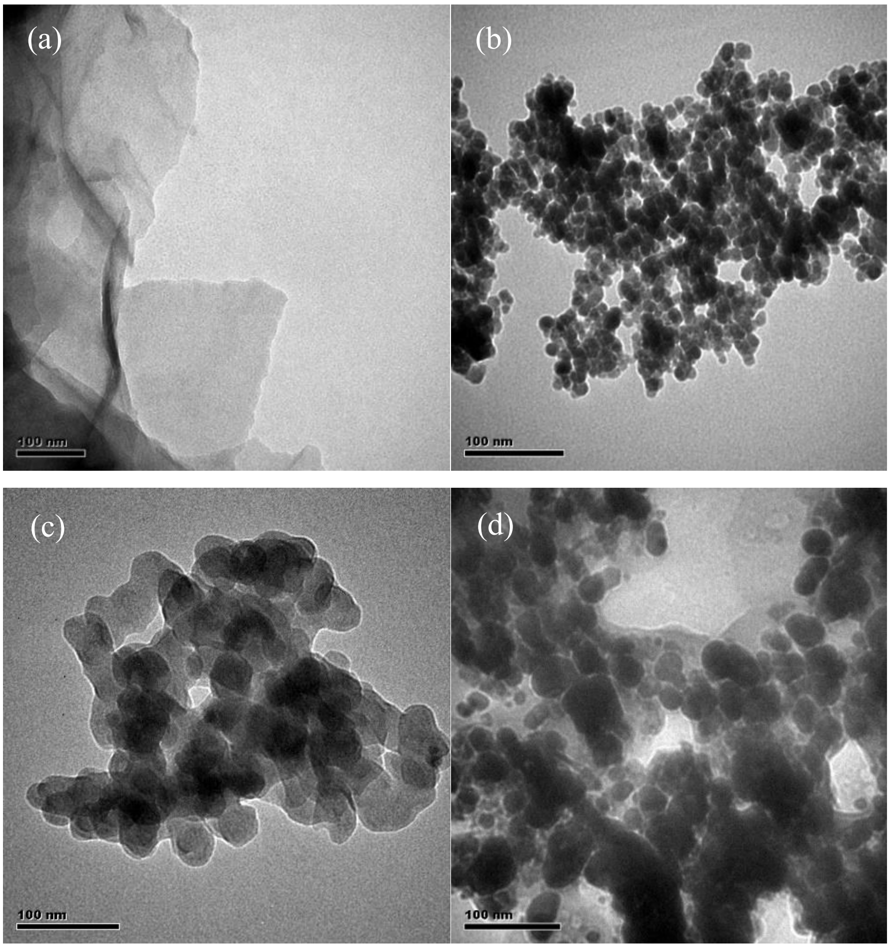

Fig.1. TEM images of GO (a), Fe_3O_4 NPs (b), MIL-100(Fe) (c) and GO/MIL-100(Fe)@Fe_3O_4 (d).

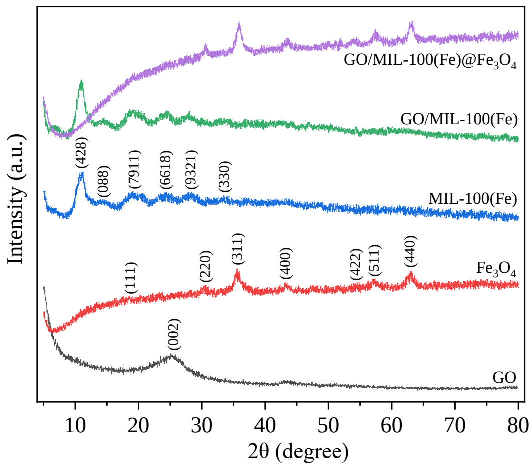

Fig.2. XRD patterns of GO, Fe_3O_4 NPs, MIL-100(Fe), GO/MIL-100(Fe) and GO/MIL-100(Fe)@Fe_3O_4.

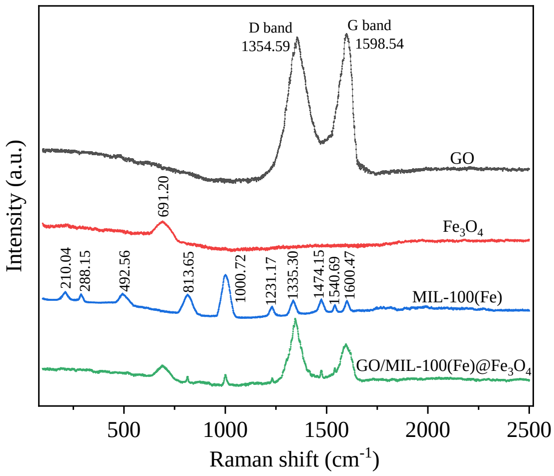

Fig.3. Raman spectra of GO, Fe_3O_4 NPs, MIL-100(Fe) and GO/MIL-100(Fe)@Fe_3O_4.

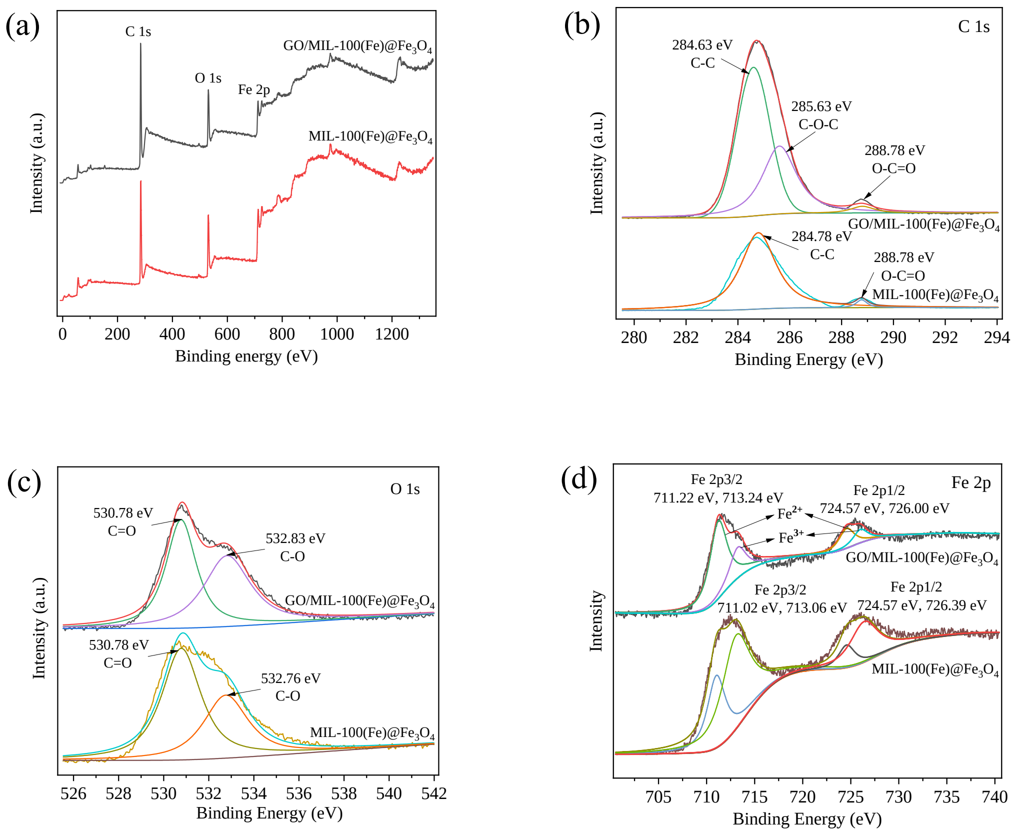

Fig.4. XPS analysis of catalysts: full-scan spectrum (a), C 1s (b), O 1s (c) and Fe 2p (d).

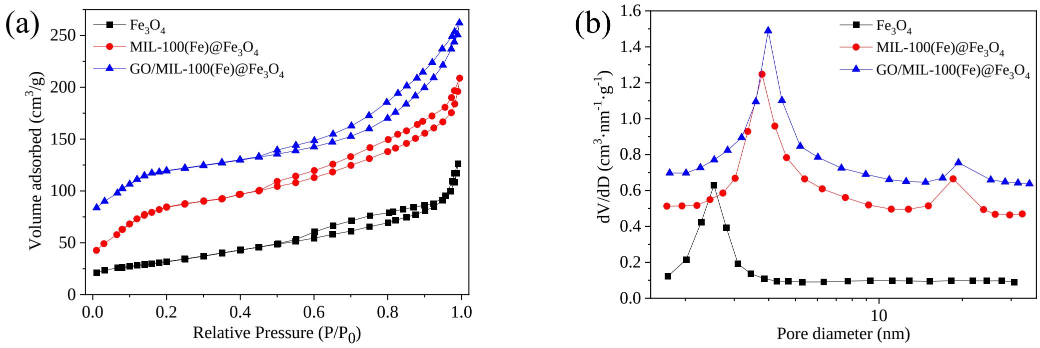

Fig.5. N_2 adsorption-desorption isotherms of Fe_3O_4 NPs, MIL-100(Fe)@Fe_3O_4 and GO/MIL-100(Fe)@Fe_3O_4 (a), and the corresponding BJH pore size distribution (b).

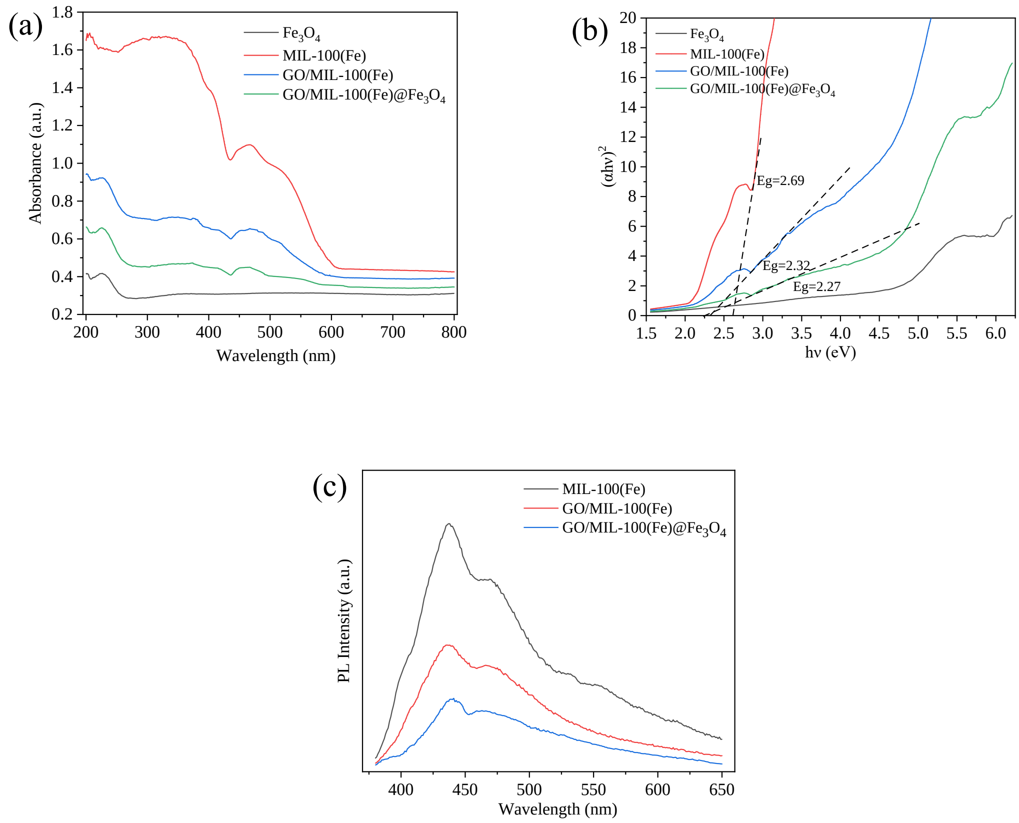

Fig.6. UV-vis diffuse reflection spectra of catalysts (a), the corresponding plots of $(ab\nu)^2$ vs. photon energy (hν) (b), and photoluminescence (PL) spectra (c).

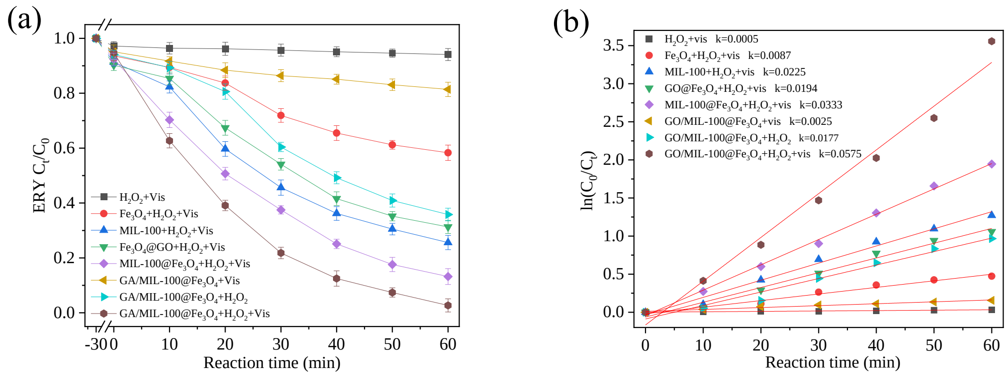

Fig.7. Degradation curves in different reaction systems (a), and the corresponding degradation kinetics of degradation curves (pseudo-first-order kinetic model) (b). pH = 4.03, $[H_2O_2]_0$ = 10 mmol/L, $[catalysts]_0$ = 0.1 g/L, $[ERY]_0$ = 0.1 mmol/L, T = 30℃.

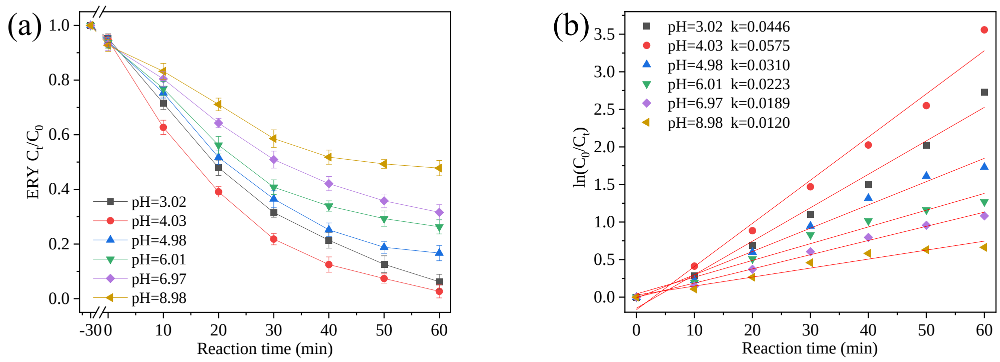

Fig.8. Effect of initial pH on ERY photo-Fenton degradation (a), and the kinetic analysis of ERY degradation at different initial pH (pseudo-first-order kinetic model) (b). $[H_2O_2]_0$ = 10 mmol/L, $[catalysts]_0$ = 0.1 g/L, $[ERY]_0$ = 0.1 mmol/L, T = 30℃.

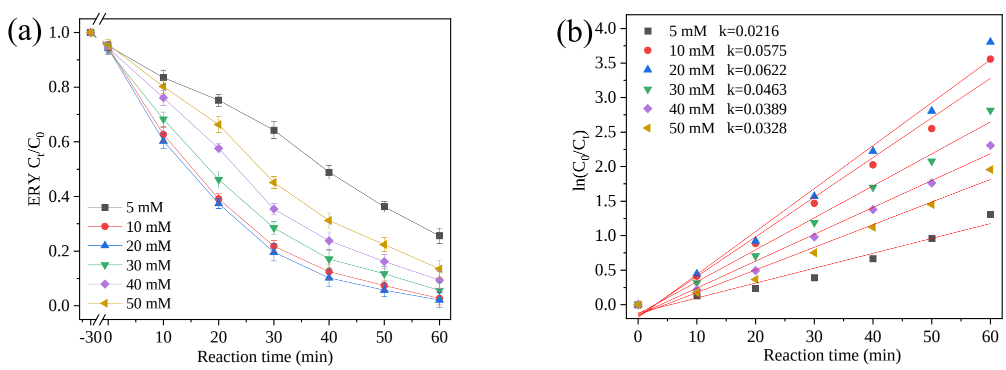

Fig.9. Effect of initial H_2O_2 concentration on ERY photo-Fenton degradation (a), and the kinetic analysis of ERY degradation at different initial H_2O_2 concentration (pseudo-first-order kinetic model) (b). pH = 4.03, $[catalysts]_0$ = 0.1 g/L, $[ERY]_0$ = 0.1 mmol/L, T = 30°C.

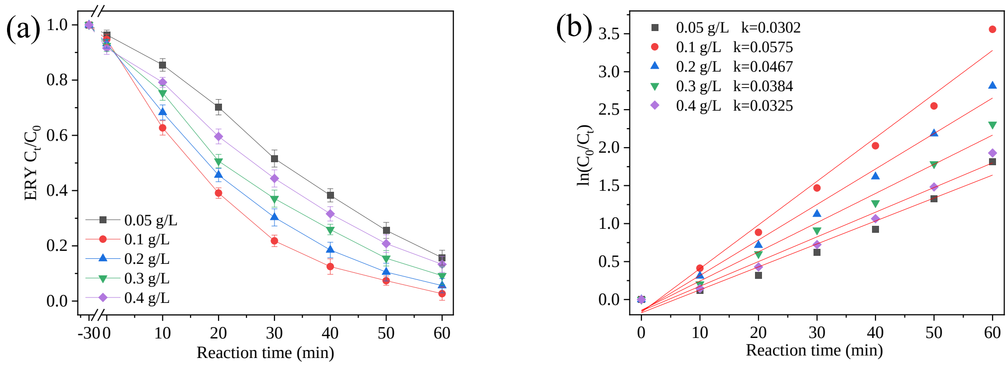

Fig.10. Effect of catalyst dosage on ERY photo-Fenton degradation (a), and the kinetic analysis of ERY degradation at different catalyst dosage (pseudo-first-order kinetic model) (b). pH = 4.03, $[H_2O_2]_0$ = 10 mmol/L, $[ERY]_0$ = 0.1 mmol/L, T = 30°C.

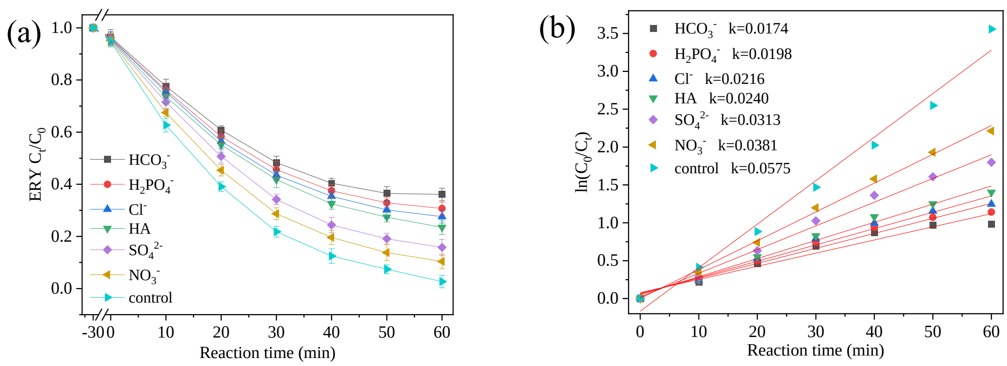

Fig.11. Effect of coexisting HA and anions on ERY photo-Fenton degradation (a), and the kinetic analysis of ERY degradation at coexisting HA and anions (pseudo-first-order kinetic model) (b). pH = 4.03, $[catalysts]_0$ = 0.1 g/L, $[H_2O_2]_0$ = 10 mmol/L, $[ERY]_0$ = 0.1 mmol/L, [HA] = 10 mg/L, [anions] = 10 mg/L, T = 30°C.

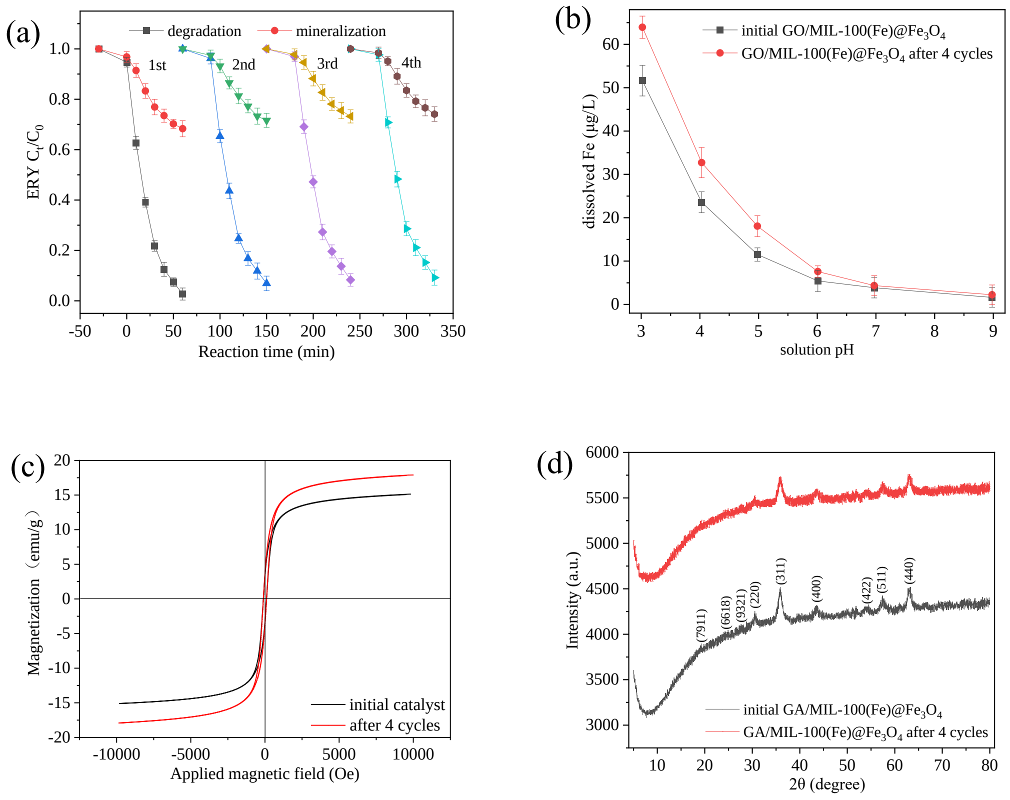

Fig.12. Cycling runs of ERY degradation in the photo-Fenton system (a), leaching of Fe during 1st cycle and 4th cycles (b), magnetic hysteresis loop at 298 K (c) and XRD patterns (d) of initial GO/MIL-100(Fe)@Fe_3O_4 and after 4 cycles under the optimum conditions. pH = 4.03, $[H_2O_2]_0$ = 10 mmol/L, $[\text{catalysts}]_0$ = 0.1 g/L, $[\text{ERY}]_0$ = 0.1 mmol/L, T = 30°C.

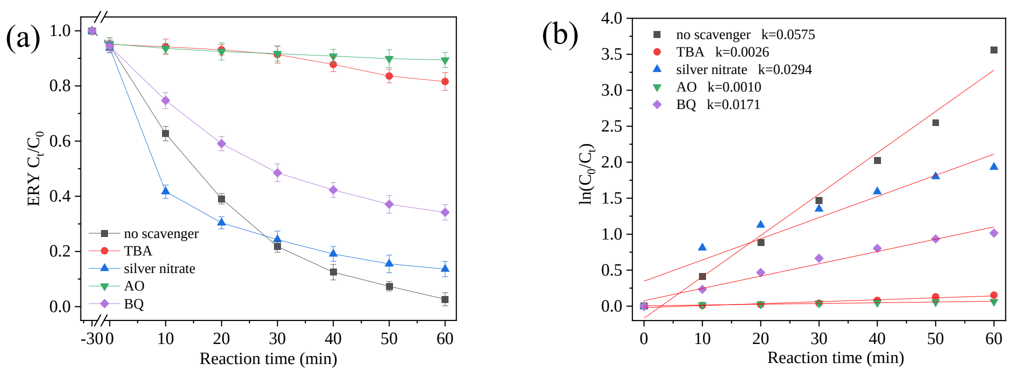

Fig.13. Effect of radical scavengers on ERY degradation in photo-Fenton (a), and the

kinetic analysis of ERY degradation at different radical scavengers (pseudo-first-order kinetic model) (b). pH = 4.03, $[H_2O_2]_0$ = 10 mmol/L, $[catalysts]_0$ = 0.1 g/L, $[ERY]_0$ = 0.1 mmol/L, T = 30°C.

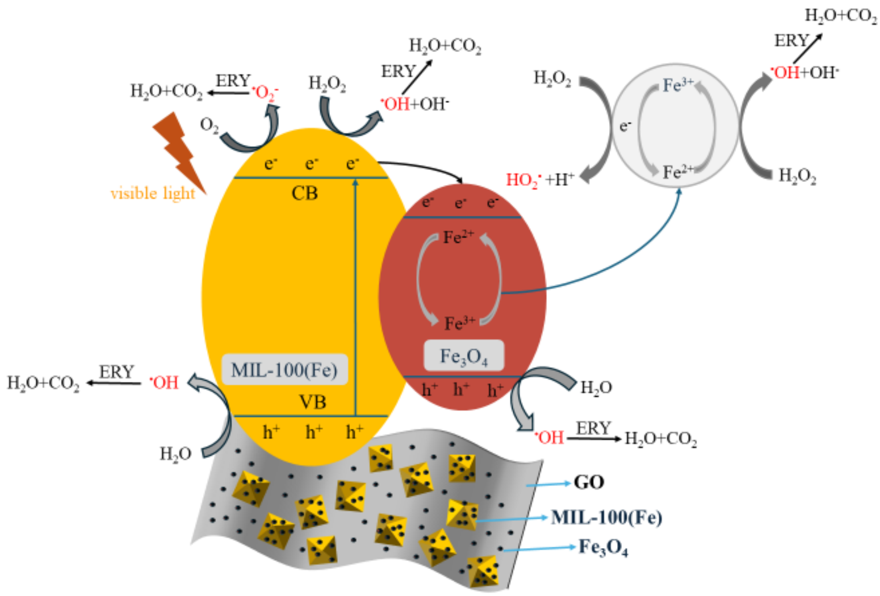

Fig.14. The proposed degradation mechanism of ERY in photo-Fenton system over GO/MIL-100(Fe)@Fe_3O_4.